JOURNAL OF CATALYSIS **163,** 106–116 (1996)
ARTICLE NO. 0309

Effect of Pore Geometry on Ring Closure Selectivities in Platinum L-Zeolite Dehydrocyclization Catalysts

J. T. Miller,[1] N. G. B. Agrawal, G. S. Lane, and F. S. Modica

Amoco Research Center, 150 W. Warrenville Road, P.O. Box 3011, Mail Station H-9, Naperville, Illinois 60566-7011

Received February 20, 1996; revised May 24, 1996; accepted May 29, 1996

Experimental evaluations of nonacidic supported platinum catalysts for the conversion of *n*-hexane to benzene demonstrate that the support geometry plays a major role in controlling the primary amount of benzene formed relative to methylcyclopentane, or the 1–6 to 1–5 ring closure selectivity. For most catalysts including nonacidic zeolite and amorphous supports, the 1–6 to 1–5 ring closure selectivity is about 0.5. However, Pt/K–LTL catalysts exhibit a ring closure selectivity greater than 1.0. In addition, increasing the alkali level above the ion-exchange capacity of the zeolite increases the ring closure selectivity slightly. Although the C_1–C_5 hydrogenolysis selectivity is determined primarily by the inherent properties of the metal, a small excess of alkali was also important for optimum reduction of the hydrogenolysis selectivity. The catalyst selectivities are discussed with respect to the models proposed in the literature which account for the high benzene yield of Pt/K–LTL compared to other catalysts. The experimental results are most consistent with the preorganization model, in which the reactant molecule is adsorbed in the zeolite channel in a conformation which is similar to the transition state, leading to a perference for 1–6 ring closure. The significance of 1–6 to 1–5 ring closure selectivity was demonstrated via computer simulations of the reaction pathway of *n*-hexane to benzene. The simulations demonstrate that a high 1–6 to 1–5 ring closure selectivity leads to a higer apparent activity at high *n*-hexane conversions. In addition, at high conversion a catalyst with high ring closure selectivity gives almost double the benzene yield at constant C_1–C_5 yield. These differences are important in the selection of a catalyst for commercial application and make the Pt/K–LTL catalyst with small platimum particles and a slight excess of alkali the clear choice.

INTRODUCTION

Platinum clusters in alkaline LTL zeolite are highly active and selective for the dehydrocyclization of straight-chain paraffins into aromatics (1–4). Research on these catalysts has led to the commercial development of a new nephtha reforming process for production of benzene for the petrochemical industry (5, 6). Several explanations have been proposed to account for the high aromatic yields of this catalyst. There is general agreement that the dehydrocyclization mechanism is monofunctional depending only on the Pt sites (2, 4, 7). In addition, in order to avoid yield loss by acid-catalyzed isomerization and hydrocracking, the support must be non-acidic (2, 8). Several groups, however, have demonstrated that the more basic the LTL zeolite, the higher the aromatic selectivity. The interaction of the Pt particles with the basic support is thought to result in an increase in the electron density of the Pt leading to a modification of its adsorptive (9, 10) and catalytic properties (11–16).

While electronic modifications of the Pt appear to contribute to the catalyst performance, the steric environment of the Pt clusters may also be important. One explanation suggests that the small pore openings in zeolites orient the reacting *n*-paraffin such that the initial adsorption is at the terminal carbon (17). Terminal adsorption leads to a higher probability of 1–6 ring closure and a higher aromatic selectivity. In addition, terminal adsorption will favor hydrogenolysis at the terminal carbon atom yielding, for example, methane and *n*-pentane from *n*-hexane. A high probability for terminal adsorption was characteristic of Pt on high-silica-faujasite and alkaline LTL. Collimation effects have also been demonstrated for ring opening of methlycyclopentane where the spacial confinement of the LTL pore structure orients the methyl group parallel to the pore axis increasing the 3-methylpentane and *n*-hexane selectivity (18). Catalysts with high terminal adsorption for *n*-paraffins, however, have been observed with amorphous catalysts where steric effects would not be expected to exist (7, 8). While there was a general correlation of increased aromatic selectivity over catalysts with increased terminal adsorption, it was concluded that the increased selectivity for terminal adsorption was not due to the mircoporous nature of zeolite supports, but was rather an intrinsic property of platinum on nonacidic supports (8).

Based on molecular modeling, an alternative geometric explanation has been proposed where optimization of the van der Waals forces between the pore walls and the adsorbed *n*-parafin leads to cyclic adsorption, similar in conformation to the transition state required for aromatic formation. Preorganization of the transition state by the pore

[1] To whom correspondence should be addressed. E-mail: jmiller@amoco.com.

0021-9517/96 $18.00

walls was thought to be responsible for the high aromatic selectivity of the Pt/K–LTL catalyst (19). Experimentally, an increase in the one-six to one-five ring closure ratio is observed for conversion of *n*-hexane to benzene by Pt/K–LTL compared to Pt/K–FAU, Pt/K–Al_2O_3, and Pt/SiO_2 (7). The same group which proposed the pre-organizational model, however, later ruled-out the importance of geometric and adsorptive effects of the LTL zeolite since similar aromatization selectivities were obtained for Pt supported on basic, magnesia-alumina hydrotalcite clay (20–22).

The influence of micropore geometry has also been proposed to inhibit deactivation of the Pt clusters. Within the narrow pores of the zeolite, bimolecular reactions leading to carbon deposition are inhibited. The high aromatic selectivity is thought to be characteristic of a clean Pt surface (23). Finally, high benzene selectivities have also been demonstrated for other Pt zeolite and amorphous catalysts. The increased aromatic selectivity, however, was attributed to the low hydrogenolysis activity of Pt particles smaller than about 1 nm, rather than to the specific pore geometry (8). Despite the numerous studies, there is limited evidence indicating that the LTL pore geometry contributes to the enhanced aromatization selectivity.

In this paper, evidence is presented which indicates that Pt/K–LTL displays an enhanced 1–6 ring closure selectivity compared to other nonacidic zeolite and amorphous Pt aromatization catalysts. In addition, modeling of the reaction pathway demonstrates that the increased 1–6 ring closure selectivity of Pt/K–LTL leads to higher activity and aromatic selectivity, especially, at high conversions typical of commercial operations.

EXPERIMENTAL

Catalyst Preparation

The zeolite supports were commercial samples or were synthesized. Na–Y (FAU), and K–L (LTL) zeolities were commercial samples obtained from UOP. Na-Ferierite (FER) (24), Na–ZSM-5 (MFI) (25), Na–ZSM-12 (MTW) (26), Na–Omega (MAZ) (27), and Na–Beta (BEA) (28) zeolites were synthesized following published procedures. For zeolites prepared with organic amines, the zeolites were calcined in air at 813 K for 16 h. All zeolites (except LTL) were ion exchanged with KNO_3. Typically, 75 g of zeolite was exchanged with 0.5 l of 1.5 *M* KNO_3 at 353 K for 4 h. The exchanged zeolite was filtered, washed with 0.5 l cold H_2O and refiltered. The potassium-exchanged zeolite was given a second wash with 0.5 l of dilute KOH. The pH of the second wash was adjusted to 9.5 with KOH. The zeolite was filtered, dried, and calcined at 813 k for 3 h.

The alkali level on K–LTL and K(Na)–FAU was adjusted by repeated washing with water or by impregnation of excess alkali with KNO_3. Each support was calcined at 813 K. The zeolites are designated by the cation type, International Zeolite Association structure type and the cation-to-aluminum molar ratio in parenthesis, for example, K–LTL (1.19). Elemental analyses for K, Na, Al and the cation-to-aluminum molar ratio are given in Table 1. For all zeolite catalysts, the acid sites have been neutralized by potassium exchange with a slight excess of alkali.

TABLE 1

Elemental Analysis

Catalyst support	wt% K	wt% Na	wt% Al	Cation/Al (molar ratio)
K–FER	3.29	nd	2.27	1.00
K–MFI	2.28	nd	1.35	1.16
K–MTW	1.45	nd	0.99	1.01
K–BEA	4.10	nd	2.58	1.10
K–MAZ	11.0	nd	7.00	1.08
K–LTL(1.00)	11.8	nd	8.2	1.00
K–LTL(1.05)	12.5	nd	8.2	1.05
K–LTL(1.19)	14.6	nd	8.5	1.19
K–FAU(1.04)	10.2	3.1	10.1	1.04
K–FAU(1.11)	11.4	3.0	10.2	1.11
K–FAU(1.28)	13.6	3.1	10.2	1.28

Note. nd, not detected.

Alkalized silica was prepared by addition of a large excess of dilute KOH added to silica (PQ Corporation, 215 m^2/g and pore volume = 1.0 cc/g). The pH of the KOH was maintained at 9.5. The support was filtered, dried and calcined at 813 k for 3 h. The alkalized silica contained 0.82 wt% K.

Spray-dried pseudo-boehmite microspheres were calcined at 673 K. The BET surface area of the alumina was 366 m^2/g with a pore volume of 0.41 cc/g. The calcined alumina was impregnated with KNO_3 (1.6 wt% K) and recalcined at 673 K.

The magnesium-aluminum hydrotalcite clay was synthesized following published procedures (29). The MgO/Al_2O_3 molar ratio was 6.8, and the support contained 0.02 wt% K. The support was calcined at 873 K for 6 h. The hydrotalcite structure was confirmed by X-ray diffraction, and the support had a BET surface area of 218 m^2/g with a pore volume of 0.88 cc/g.

To each support, platinum was impregnated using an aqueous solution of tetraammineplatinum (II) nitrate to a weight loading of 1.0% Pt. The platinum-impregnated catalysts were calcined in air at 533 K.

Transmission electron micrographs were obtained on thin sections of several zeolite catalysts (not shown) and indicated that there were no large Pt particles external to the zeolite pores. The only visible Pt particles were within the zeolite pores, approximately filling those pores (7, 30).

Catalyst Testing

Each catalyst was tested for conversion of *n*-hexane to benzene at atmospheric pressure in a bench-scale, fixed-bed continuous flow reactor. The reactor consisted of a 0.8 cm

ID quartz tube with an internal thermocouple. The experiments were conducted using between 0.05 and 0.25 g of catalyst combined with α-alumina to give a total loading of 2 g. Both the catalyst and the α-alumina were screened to 20/45-mesh granules, and were supported on a bed of quartz wool. The reactor was operated under flowing hydrogen, and *n*-hexane (Aldrich, 99.6+% purity) was added by saturation of hydrogen through a bubbler at wet-ice temperature. In all experiments, the H_2/n-C_6H_{14} molar ratio of the feed was constant at 16. Prior to each experiment, the catalyst was reduced at 773 K in flowing hydrogen (0.2 l/min) for 1 h. the product selectivity was determined at 673 K. The *n*-hexane conversion was less than 10%, and no measurable deactivation was observed during the tests for any of the alkaline catalysts. Control experiments with only the α-alumina showed no measurable conversion.

Computer Simulations

In order to demonstrate the effects of the ring closure ratio on the catalytic performance, a simple model was formulated to simulate the reaction network depicted in Fig. 1 (4, 7). The only adjustable parameter in the model was the ring closure ratio. In one simulation, the ring closure ratio was 1.25 which is typical of Pt/K–LTL, while in the second simulation the ratio was 0.5, typical of a nonacidic Pt catalysts, for example Pt/K–FAU. The computer simulations consisted of numerically integrating along the length of an isothermal, plug flow reactor. The system was well behaved, and the results were independent of the method of integration. In order that the differences in the conversion and selectivity in the two simulations is due only to the differences in ring closure ratio, the reaction network was modeled making the following assumptions:

1. Reactions 1–4 (Fig. 1) were considered to be reversible and were assumed to follow simple, non-Langmuir, first order kinetics.

2. The turnover frequency (TOF) for *n*-hexane reacting was assumed to be the same and equal to 1.0 for both Pt/K–LTL and Pt/K–FAU. That is, the sum of the rate coefficients for 1–6, 1–5 ring closure and hydrogenolysis products from *n*-hexane was equivalent in both simulations, i.e., $k_4 + k_1 + k_5 = 1.0$.

3. The initial hydrogenolysis selectivity $[k_5/(k_1 + k_4 + k_5)]$ was assumed to be 0.05 for both catalysts.

4. Hydrogenolysis was assumed to be irreversible, and the rate constant for all C_6 saturates, except methylcyclopentane, were assumed to be equal, i.e., $k_5 = 0.05$. Methylcyclopentane was assumed not to react to C_1–C_5 products. (Results not presented here were insensitive to this assumption.)

5. Ring opening of methylcyclopentane was assumed to produce only *n*-hexane, 2-methylpentane and 3-methylpentane in the statistical 2 : 2 : 1 ratio.

With these assumptions and using the equilibrium constants, rate constants for the reverse reactions were calculated. Table 2 summarises the rate coeficients used in the two simulations. The increase in hydrogen partial pressure due to dehydrocyclization and the overall expansion due to the increase in the number of moles was neglected. Other inlet conditions were as follows and were assmed to be constant through the reactor: temperature 673 K, 1 atm total pressure, and H_2/n-hexane feed mole ratio of 16.

The simulation included the following equations for each component:

Component	Rate equation
*n*Hx	$-(k_1 + k_4 + k_5)^*[n\text{Hx}] + k^*_{-1}[\text{MCP}] + k^*_{-4}[\text{Bz}]$
MCP	$-(k_{-1} + k_{-2} + k_{-3})^*[\text{MCP}] + k^*_1[n\text{Hx}] + k^*_2[\text{2MP}] + k^*_3[\text{3MP}]$
2MP	$-(k_2 + k_5)^*[\text{2MP}] + k^*_{-2}[\text{MCP}]$
3MP	$-(k_3 + k_5)^*[\text{3MP}] + k^*_{-3}[\text{MCP}]$
Benzene	$k^*_4[n\text{Hx}] - k^*_{-4}[\text{Bz}]$
C_{5-}	$k^*_5\{[n\text{Hx}] + [\text{2MP}] + [\text{3MP}]\}$

TABLE 2

Rate Coefficients for the Reaction Pathway *n*-Hexane to Benzene[a]

Catalysts	Pt/K–LTL[b]	Pt/K–FAU[b]
1–6/1–5 ring closure ratio (k_4/k_1)	1.25	0.5
Rate constants (reaction)		
k_1 (*n*Hx → MCP)	0.422	0.633
k_{-1} (MCP → *n*Hx)	1.11	1.681
k_2 (2MP → MCP)	0.275	0.417
k_{-2} (MCP → 2MP)	1.11	1.681
k_3 (3MP → MCP)	0.273	0.41
k_{-3} (MCP → 3MP)	0.56	0.841
k_4 (*n*Hx → Bz)	0.527	0.317
k_{-4} (Bz → *n*Hx)	0.0095	0.0057
k_5 (*n*Hx, 2MP, 3MP → C_1–C_5)	0.050	0.050

[a] See Fig. 1 for the reaction pathway.
[b] $k_1 + k_4 + k_5 = 1.0$.

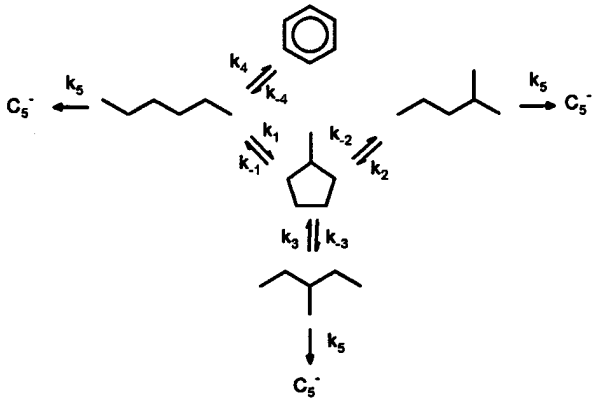

FIG. 1. Reaction network for conversion of *n*-hexane over nonacidic supported Pt catalysts.

RESULTS

Catalytic Results

Figure 1 depicts the reaction pathway for the conversion of *n*-hexane to benzene and methylcyclopentane over nonacidic platinum catalysts (4, 7). Benzene (Bz) formation occurs via 1–6 ring closure, while 1–5 ring closure leads to methylcyclopentane (MCP). Methylcyclopentane undergoes reversible ring opening to give 2-methylpentane (2MP), 3-methylpentane (3MP) or the orignal *n*-hexane (*n*Hx). Unlike bifunctional reforming catalysts, there is no direct conversion of methylcyclopentane to benzene by ring expansion and dehydrocyclization. Methylcyclopentane, 2-methylpentane and 3-methylpentane can be converted to benzene, but only by conversion back to *n*-hexane. In addition to the above ring closure reactions, hydrogenolysis of C_6 saturates produces undesirable C_1–C_5 products.

Several definitions of selectivity can be used to differentiate the catalysts. The simplest definition of benzene selectivity is the yield of benzene (in weight percent) dividend by the total conversion of *n*-hexane. Since hexane isomers (methylcyclopentane, 2-methylpentane, and 3-methylpentane) can eventually be converted to benzene, a second definition of benzene selectivity is commonly used to account for the irreversible loss of C_6 hydrocarbons. This selectivity, referred to as the ultimate benzene selectivity, is the ratio of benzene divided by benzene plus C_1–C_5 products. A third selectivity is the ring closure ratio and is defined as the yield of the one-six ring closure products (benzene) divided by the yield of products from one-five ring closure (the sum of methylcyclopentane, 2-methylpentane and 3-methylpentane).

The effect of support alkalinity, i.e., the K/Al molar ratio, on C_1–C_5 hydrogenolysis selectivity and ring closure ratio was determined for Pt/LTL and Pt/FAU catalysts (Table 3). In general, catalysts with an excess of alkali above the ion-exchange capacity have lower hydrogenolysis selectivities than those with a K/Al ratio near 1.0. A further increase in alkali, however, has little additional effect. For example, increasing the K/Al ratio in K–LTL from 1.00 to 1.05 reduces C_1–C_5 selectivity from 0.13 to 0.04, but a further increase in the K/Al ratio to 1.19 gives no further decrease. Similarly, Table 3 shows the hydrogenolysis selectivity of all K–FAU catalysts are approximately the same despite the increasing K/Al ratio from 1.04 to 1.28. When compared with a slight excess of alkali, e. g., K/Al = 1.05, Pt/K–LTL and Pt/K–FAU have approximately the same C_1–C_5 seletivity, 0.04 and 0.06, respectively.

Table 3 also indicates that addition of excess alkali also affects the ring closure ratio. For Pt/K–LTL, the ring closure ratio increases from 1.0 to 1.3 as the K/Al ratio increases from 1.00 to 1.19. Similarly, for Pt/K–FAU the ring closure ratio increases from 0.40 to 0.48 as the K/Al ratio increases from 1.04 to 1.28. While increasing the alkali level increases the ring closure ratio for both catalysts, the ring closure ratio for Pt/K–LTL remains substantially higher than that for Pt/K–FAU. Thus, the different ring closure ratios in Pt/K–LTL and Pt/K–FAU cannot be explained by the differences in the support alkalinity.

Since Pt/K–LTL and Pt/K–FAU have similar hydrogenolysis selectivities, the effect of a higher ring closure ratio is to increase benzene selectivity. At constant conversion, Pt/K–LTL produces more benzene than Pt/K–FAU. For the former the benzene selectivity is approximately 0.5, and the latter is 0.3 (Table 3). Compared at constant benzene yield, rather than at constant *n*-hexane conversion, the C_1–C_5 yield of Pt/K–LTL is lower resulting in a higher ultimate benzene selectivity. The direct effect of a higher ring closure ratio, therefore, is to increase the ultimate benzene selectivity from about 0.8 in Pt/K–FAU to 0.9 in Pt/K–LTL.

Table 4 lists the selectivities for several amorphous and zeolite catalysts with widely varying support geometries. Alkali levels of all the zeolite catalysts were adjusted to K/Al = 1.0–1.2 (see Table 1). In addition, small amounts of potassium were added to the sliica and alumina supports. Except for small pore zeolites, the C_1–C_5 hydrogenolysis selectivities for most of these catalysts were similar, and in

TABLE 3

***n*-Hexane Product Selectivities**[a]

Catalyst support (1.0 wt% Pt)	Pt dispersion[b] (H/Pt)	C_1–C_5	*i*-Hexanes	Benzene	Ultimate benzene	Ring closure (1–6/1–5)
K–LTL(1.00)	0.55	0.13	0.45	0.43	0.77	0.96
K–LTL(1.05)	0.78	0.04	0.46	0.50	0.93	1.09
K–LTL(1.19)	1.15	0.04	0.41	0.55	0.93	1.34
K–FAU(1.04)	0.45	0.06	0.67	0.27	0.82	0.40
K–FAU(1.11)	0.40	0.07	0.66	0.27	0.79	0.41
K–FAU(1.28)	0.41	0.11	0.60	0.29	0.73	0.48

[a] 10% *n*-hexane conversion, 673 K, atmospheric pressure and $H_2/n\text{-}C_6H_{14} = 16$.
[b] Based on H_2 chemisorption.

TABLE 4

***n*-Hexane Product Selectivities**[a]

Catalyst support (1.0 wt% Pt)	Pt dispersion[b] (H/Pt)	C_1–C_5	*i*-Hexanes	Benzene	Ultimate benzene	Ring closure (1–6/1–5)
K–FER	0.51	0.54	0.32	0.14	0.21	0.46
K–MFI	0.56	0.20	0.51	0.29	0.59	0.57
K–MTW	0.28	0.15	0.57	0.28	0.65	0.50
K–BEA	0.55	0.13	0.56	0.31	0.70	0.55
K–MAZ	0.66	0.11	0.47	0.42	0.79	0.89
K–LTL(1.19)	1.15	0.04	0.41	0.55	0.93	1.34
K–FAU(1.11)	0.40	0.07	0.66	0.27	0.79	0.41
SiO_2	0.40	0.12	0.67	0.21	0.64	0.31
K–SiO_2 (0.82 wt% K)	0.88	0.12	0.60	0.28	0.70	0.47
Al_2O_3	0.82	0.17	0.61	0.22	0.56	0.36
K–Al_2O_3 (1.6 wt% K)	0.91	0.07	0.64	0.29	0.81	0.45
MgO–Al_2O_3 (hydrotalcite clay)	0.11	0.08	0.77	0.15	0.65	0.19

[a] 10% *n*-hexane conversion, 673 K, atmospheric pressure and $H_2/n\text{-}C_6H_{14} = 16$.
[b] Based on H_2 chemisorption.

the range of 0.04–0.13. The hydrogenolysis selectivities for the small pore zeolites (MTW, MFI, FER) were significantly higher, ranging from 0.20–0.54. Also, the C_1–C_5 selectivity for the non-alkali promoted Pt/Alumina catalyst was higher at 0.17, but dropped to 0.07 on addition of alkali.

Ring closure ratios were in the range of 0.4–0.6 for all alkaline zeolite catalysts except Pt/K–LTL and Pt/K–MAZ which were significantly higher. Ring closure ratios for non-alkaline Pt/silica and Pt/alumina were slightly lower than 0.4, but increased on addition of alkali to the range of the alkaline zeolite catalysts. Despite its strongly basic support, the Pt/MgO–Al_2O_3 catalyst had the lowest ring closure ratio, 0.2. Among the catalysts examined, the high ring closure ratios of Pt/K–LTL and Pt/K–MAZ appear to be unique.

As discussed above for Pt/K–LTL and Pt/K–FAU, the direct effect of increasing the ring closure ratio is to increase the benzene and ultimate benzene selectivities. For example, even though the C_1–C_5 hydrogenolysis selectivity of Pt/MgO–Al_2O_3 (0.08) is slightly lower than that of Pt/K–MAZ (0.11), because the ring closure ratio of the former is lower, the ultimate benzene selectivity is lower, 0.65 compared to 0.79 for Pt/K–MAZ. Even small changes in the ring closure ratio produce significant improvements. For example, addition of alkali to Pt/SiO_2 has no effect on the C_1–C_5 hydrogenolysis selectivity, but increases the ring closure ratio from 0.31 in Pt/SiO_2 to 0.47 in Pt/K–SiO_2 resulting in an increased ultimate benzene selectivity from 0.64 to 0.70, respectively. A similar trend is demonstrate for Pt/Al_2O_3 and Pt/K–Al_2O_3. Finally, while the ring closure ratio is an important selectivity, it is not the only requirement for a selective aromatics catalyst. The ring closure ratio of Pt/K–FER and Pt/K–SiO_2 are nearly equivalent, ca. 0.46, however, because of the high hydrogenolysis selectivity of Pt/K–FER (0.54), the ultimate benzene selectivity is low (0.21). In the case of Pt/K–FER, it appears that small size of the pores inhibits the formation of the methylcyclopentane and benzene transition states. As a result, hydrogenolysis is favored over the ring closure reactions. With Pt/K–FER, the C_1–C_5 selectivity dominates the benezene and ultimate benzene selectivities. The effect of increasing the ring closure ratio (in any catalyst) is to improve the benzene selectivity. However, even a very high ring closure ratio could not overcome the very high C_1–C_5 hydrogenolysis selectivity of the Pt/K–FER catalyst.

Terminal adsorption of *n*-hexane on Pt has been proposed to lead to 1–6 ring closure with the formation of benzene. The terminal cracking index (TCI), defined as the molar ratio of *n*-pentane to *n*-butane in the C_1–C_5 products, has been proposed as a measure of terminal adsorption (17). The relationship between the ring closure ratio and the TCI for the catalysts in this stdy is shown in Fig. 2. Despite the wide variation in TCI, no correlation between TCI and the ring closure ratio is evident. In particular, Pt/K–LTL has a higher ring closure ratio (1.3) than catalysts with a similar TCI, such as Pt/K–MTW, Pt/K–MFI, Pt/K–BEA, and Pt/K–SiO_2 (0.4–0.6). Conversely, Pt/K–FAU has a much higher TCI than Pt/K–BEA, Pt/K–SiO_2 and Pt/K–Al_2O_3, but a similar ring closure ratio. The higher ring closure ratios of Pt/K–LTL and Pt/K–MAZ, therefore, are not related to the TCI.

Computer Simulations

In order to demonstrate the effect of the ring closure ratio on the product selectivity and conversion, computer

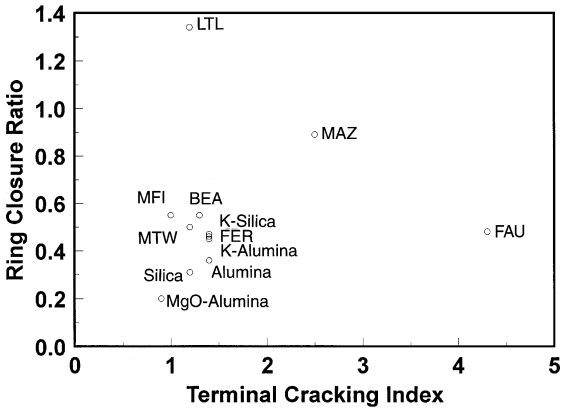

FIG. 2. Terminal cracking index (mole ratio of *n*-pentane/*n*-butane) versus ring closure ratio (1–6 ring closure selectivity/1–5 ring closure selectivity).

simulations for conversion of *n*-hexane to benzene were conducted. Fig. 3 illustrates the results of the effect of the ring closure ratio on *n*-hexane conversion. For simple first order kinetics, a plot of ln(1-conv), or ln(*n*-hexane remaining), versus reactor length is linear. However, in Fig. 3 as the amount of *n*-hexane remaining decreases (conversion increases), the magnitude of the slope of the lines decrease, indicating that the rate of disappearance of *n*-hexane is lower than would be expected from a simple first order reacion. The curvature is a consequence of the presence of two kinetic regimes. At low conversions, the reaction of *n*-hexane to its primary products (benzene, methylcyclopentane and C_1–C_5 products) is rate controlling. In these simulations, the initial rate of *n*-hexane conversion was chosen to be the same in both simulations, thus the initial slopes are the same. As the conversion of *n*-hexane increases, the concentrations of 2-methylpentane and 3-methylpentane increase. At high conversion, methylcyclopentane approaches equilibrium with its ring opening products, *n*-hexane, 2-methylpentane and 3-methylpentane. The reverse reaction of 2-methylpentane and 3-methylpentane to produce *n*-hexane (through methylcyclopentane) becomes rate determining for the formation of benzene. The conversion of 2-methylpentane and 3-methylpentane to benzene requires three reactions, 1–5 ring closure to produce methylcyclopentane, ring opening to yield *n*-hexane and 1–6 ring closure of hexane to give benzene. The rate of benzene formation from secondary products (2-methylpentane and 3-methylpentane) is slower than the rate of formation of benzene directly from *n*-hexane.

The *n*-hexane concentration at which the conversion of 2-methylpentane and 3-methylpentane becomes rate limiting is determined by the ring closure ratio. A lower the ring closure ratio (higher 1–5 ring closure rate) leads to higher concentration of 2-methylpentane and 3-methylpentane. Hence, the rate of benzene formation from these products becomes rate determining at a higher *n*-hexane concentration than for a catalyst with the lower ring closure ratio. Figure 3 shows this with the two simulations at different ring closure ratios diverging at different *n*-hexane conversions. Although the *n*-hexane conversions differ by only a few per cent at conversions above 90%, approximately half the reactor length is required to obtain the same *n*-hexane conversion for Pt/K–LTL as Pt/K–FAU. For example, the reactor length required for 95% conversion of *n*-hexane is approximately 0.35 for Pt/K–LTL, but 0.70 for Pt/K–FAU. Thus, at high conversion, the catalyst with a higher ring closure ratio requires significantly less reactor volume, i.e., less catalyst, to obtain the same conversion compared to a catalyst with the same initial TOF, but a lower ring closure ratio.

Figure 4 shows the effect of ring closure ratio on the ultimate benzene selectivity, Benzene/(Benzene + C_1–C_5). The

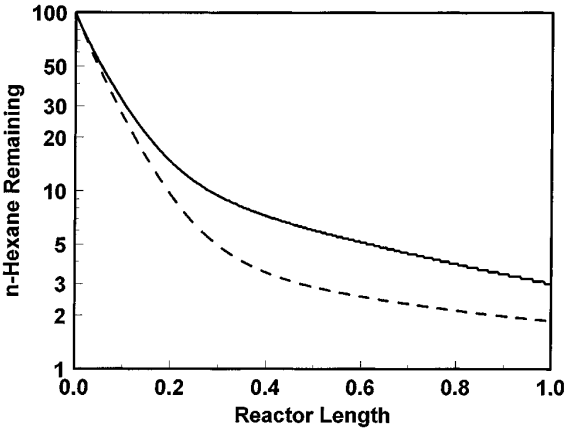

FIG. 3. Computer simulation for conversion of *n*-hexane versus reactor length, solid line: ring closure ratio 0.5, and dotted line: ring closure ratio 1.25.

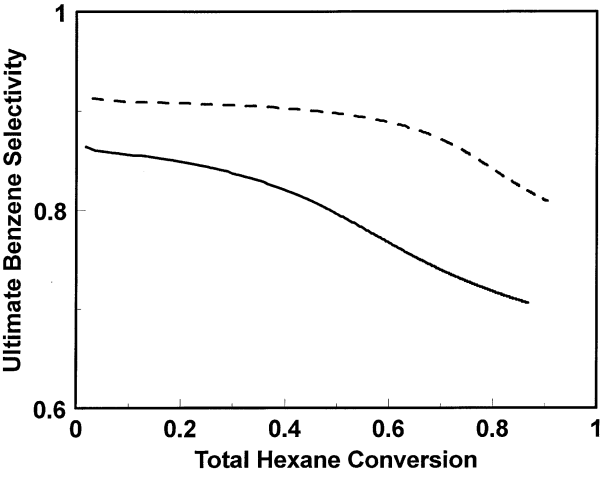

FIG. 4. Computer simulation of ultimate benzene selectivity versus total hexane conversion (total hexane is the sum of *n*-hexane, methylcyclopentane, 2-methylpentane and 3-methylpentane), solid line: ring closure ratio 0.5, and dotted line: ring closure ratio 1.25.

selectivity at low conversion is equal to the ratio of rate coefficients, $k_4/(k_4 + k_5)$. Since k_4 was chosen to be higher for the P/K–LTL simulation, the initial benzene selectivity is higher. In both cases, as the conversion increases, the benzene selectivity decreases slightly. As conversion increases, some *n*-hexane is converted to 2-methylpentane and 3-methylpentane. Since 2-methylpentane and 3-methylpentane undergo some hydrogenolysis and cannot form benzene directly, the benzene selectivity decreases. The ratio of 2-methylpentane and 3-methylpentane to *n*-hexane increases with increasing conversion and increases very rapidly at high conversion. As a result, the ultimate benzene selectivity decreases more rapidly at high conversion. Decreasing the ring closure ratio, or increasing the 1–5 ring closure rate, results in higher 2-methylpentane and 3-methylpentane concentrations resulting in higher hydrogenolysis rates. In these simulations, the initial ultimate benzene selectivity for Pt/K–LTL is about 5% higher than that of Pt/K–FAU, 0.91 and 0.86, respectively, but this increases to about 13%, for example, 0.84 vs 0.71 at 80% conversion of all hexanes.

While these diferences in selectivity might, at first, seem small, they have a large effect on the yields of benzene and C_1–C_5 products, as shown in Fig. 5. Initially, C_1–C_5 yields increase linearly with the benzene yield. The initial slope is equal to the ratio of the rate coefficients for hydrogenolysis and formation of benzene, k_5/k_4. Since the 1–6 ring closure rate coefficient was specified to be larger for Pt/K–LTL, the initial slope of Pt/K–LTL is lower than that of Pt/K–FAU, i.e., the C_1–C_5 yields are lower for Pt/K–LTL than Pt/K–FAU at a constant benzene yield. As conversion increases, both curves bend upward corresponding to an increase in C_1–C_5 product for a given increase in benzene yield. The change in slope corresponds to the point where the hydrogenolysis of 2-methylpentane and 3-methylpentane contribute to the formation of C_1–C_5 products without formation of benzene, as discussed above. The benzene yield at which these curves bend upward is determined by the ring closure ratio.

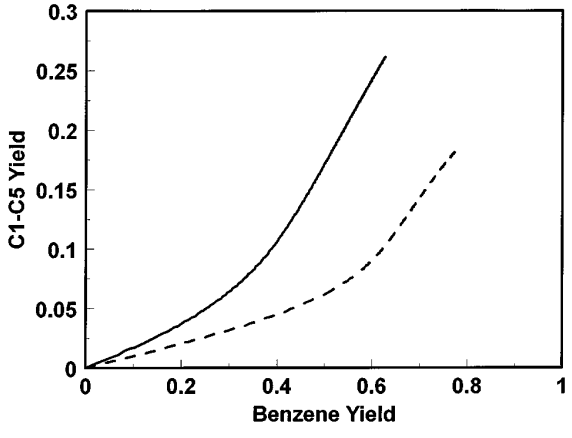

FIG. 5. Computer simulation of C_1–C_5 yield versus benzene yield, solid line: ring closure ratio 0.5, and dotted line: ring closure ratio 1.25.

In commercial practice, the economics of the process is often determined by the amount of low valued byproducts (C_1–C_5) and the yield of benzene that can be produced at that C_1–C_5 yield. As shown in Fig. 5, Pt/K–LTL produces significantly more benzene at a given C_1–C_5 yield than Pt/K–FAU. For example, at 0.10 C_1–C_5 yield, the benzene yield for Pt/K–FAU is 0.39. In contrast, Pt/K–LTL has a 0.62 benzene yield at the same 0.10 yield of C_1–C_5 products. This difference in benzene yield is due to the different ring closure ratios since hydrogenolysis selectivity was identical for both catalysts. Thus, although the hydrogenolysis selectivity is an important parameter in evaluating catalysts, the ring closure ratio is equally important and must be considered in any catalyst comparison.

DISCUSSION

The results of this study demonstrate that Pt/K–LTL, and to a lesser extent Pt/K–MAZ, is unique among nonacidic aromatization catalysts. While most platinum on nonacidic supports exhibited a similar, low hydrogenolysis rate, as previously obsered by Davis (8), only Pt/K–LTL has a high 1–6 to 1–5 ring closure ratio. As shown in the simulations, at high *n*-hexane conversion, a high ring closure ratio leads to a more active catalyst and higher benzene yields.

Several models have been proposed to explain the high benzene yield of Pt/K–KTL catalysts. A number of studies have shown an improved aromatic selectivity with increasing support basicity (2, 3, 8, 11, 13, 14). For Pt/LTL catalysts, the base strength of the zeolite was increased by exchange of larger alkali cations (11, 13, 14). As the base strength of the exchanged cation increased from Li to Cs, the aromatic selectivity increased (11, 14). In addition, as the base strength of the alkali cation increased the infrared frequency of adsorbed CO on Pt decreased indicating an increase in the platinum electron density. It was suggested that the metal-support interaction between Pt with alkaline support leads to electron-rich platinum clusters which exhibit a lower hydrogenolysis selectivity with a correspondingly higher aromatization selectivity (11, 13).

Metal-support interactions have also been demonstrated for other platinum catalyzed reactions, for example, hydrogenation of benzene (9) and hydrogenolysis of paraffins (15, 16, 31). Increasing the base strength of the exchanged cation, results in a decrease in the TOF for benzene hydrogenation (9). In addition, comparison of the equlibrium adsorption constants for competitive hydrogenation of toluene and benzene for the same catalysts indicate that there is a charge transfer from the alkaline zeolite support to the platinum clusters which increases as the base strength of the exchanged ion increases.

While the base strength of the exchanged cations affects the catalytic and spectroscopic properties of metal clusters, the level of the alkali cation is equally important. As the level of alkali in Pd/LTL (15, 16, 32) and Pt/LTL (16) catalysts increases from acidic to neutral to basic, the neopentane hydrogenolysis TOF decreases. For both the Pd/LTL and Pt/LTL catalysts, as the potassium level increased the infrared frequency of adsorbed CO shifts to lower frequency and the coordination shifts from linear to bridge-bonded (16, 32). In addition, for Pd/LTL as the potassium level of the support increased, the Pd X-ray photoelectron binding energy decreased (16). Both infrared and X-ray photoelectron spectroscopies indicate that the electron density of the metals increases due to a metal-support interaction with the basic support, similar to that observed with increasing base strength of the exchanged cation.

The effect of the level of alkali on the metal-support interaction appears to be general. Increasing amounts of potassium by addition of KOH to Pt/SiO_2, for example, results in a strong decrease in the hydrogenolysis TOF of neopentane. In addition, as observed with zeolite catalysts, there is a continual decrease in the infrared frequency of adsorbed CO and a shift from linear- to bridge-bonded CO as the level of KOH increases consistent with an increase in the platinum electron density (32). The results of the present study are in general agreement with the previous studies, in that increasing support alkalinity leads to a suppression in hydrogenolysis selectivity. For Pt/LTL, hydrogenolysis selectivities are higher and ultimate benzene selectivities are lower when the K/Al ratio is less than 1.05.

In addition to the suppression of the hydrogenolysis rate, increasing support alkalinity also results in an increase in 1–6 to 1–5 ring closure ratio. As discussed above, this increase in the ring closure also increases the aromatization selectivity, especially at high conversion. It is clear that electronic effects resulting from the interaction of the Pt with basic supports contribute to improved catalyst performance, and Pt/LTL is not unique in that respect. However, it is also clear that these effects do not entirely explain the higher ring closure ratio of the Pt/LTL catalyst. Regardless of the alkali level, Pt on no other support, whether zeolite or amorphous, displays the high ring closure ratio characteristic of Pt/LTL catalysts.

It has also been proposed that high aromatic selectivity is an intrinsic property of small metal particles, and the superiority of the Pt/LTL catalyst is thought to be due to its ability to stabilize small Pt particles (8). Because hydrogenolysis is a structure sensitive reaction, a decrease in particle size is expected to lower the hydrogenolysis selectivity and increase the benzene selectivity. All the catalysts in the current study contained small (less than 2 nm) Pt particles; however, there does not appear to be a correlation between hydrogenolysis selectivity and Pt particle size when comparing catalysts with similar alkali loadings. Nor does there appear to be a correlation between Pt particle size and ring closure ratio. For example, Pt/K–LTL and Pt/K–MAZ have significantly higher ring closure ratios compared to catalysts with similar dispersion, see Tables 3 and 4. Conversely, all remaining catalysts have similar ring closure ratios despite a range in dispersions from 0.4 to 0.9. Thus, while the Pt particle size may have a small influence on C_1–C_5 hydrogenolysis selectivity, it does not appear to explain the higher ring closure ratio of the Pt/K–LTL catalyst.

From the experimental and simulation results, it is clear that the higher benzene yield of Pt/K–LTL is due to an enhancement in the rate of 1–6 ring closure. It has been suggested that the high benzene selectivity in Pt/K–LTL is due to a preferential adsorption of *n*-hexane at the terminal carbon enhancing the rate of one-six ring closure relative to 1–5 ring closure (17). The tendency for terminal adsorption was attributed to lengthwise orientation of the *n*-hexane molecule as it diffuses through the small pore openings in zeolite catalysts leading to end on attachment at the Pt surace. The terminal cracking index (TCI) was proposed as a measure of the tendency for terminal adsorption and was correlated with the benzene selectivity for Pt/K–LTL and Pt/silica. The results of the present study show that there is no general correlation between the TCI and a high ring closure ratio, Fig. 2. Furthermore, the TCI does not appear to be a fundamental property of the geometry of the support. The TCI for many Pt/zeolite catalysts is similar to that for Pt on amorphus supports. The high ring closure ratio in Pt/K–LTL (and Pt/K–MAZ) is not due to an increased tendency for terminal adsorption.

It has also been suggested that the high benzene selectivity in Pt/K–LTL is an intrinsic property of clean (coke-free) platinum surfaces (23). Similar high benzene selectivities were observed for Pt/SiO_2 and Pt/K–LTL during the first few turnovers, but the selectivity of Pt/SiO_2 declined rapidly. It was proposed that the restrictive steric environment of the microporous zeolitie channels suppressed bimolecular reactions leading to coke resulting in the maintenance of a clean platinum surace and continued high aromatics selectivity. It would seem unlikely that the LTL zeolite is unique in its ability to inhibit deactivation, and that if this model is correct then other Pt/zeolite catalysts should also show high benzene selectivity. The experimental results of this study, however, demonstrate that Pt/K–LTL is unique in its ability to promote 1–6 ring closure. Platinum supported on zeolites with pores both larger and smaller than LTL show ring closure ratios similar to platinum on amorphous supports, such as K–silica and K–alumina. In addition, Pt/K–MFI, which is known for its ability to suppress deactivation and the formation of coke, has a ring closure ratio similar to the other catalysts. Therefore, the high ring closure ratio observed with Pt/K–LTL is not a

result of a restricted deactivation and the maintenance of a clean metal surface.

From the preceding discussions it can be seen that the enhanced ring closure ratio in Pt/K–LTL cannot be attributed to differences in Pt particle size, support alkalinity, suppression of coke or tendency for terminal adsorption of *n*-hexane. In 1998, Derouane and Vanderveken proposed that the high benzene selectivity in Pt/LTL is due to the preorganization of *n*-hexane as a cyclic intermediate leading to an enhanced rate of 1–6 ring closure (19). This proposal was based on molecular modeling of adsorption of *n*-hexane in the pores of LTL zeolite. Optimization of the van der Waals interactions between the pore walls and the adsorbed *n*-hexane leads to a nonbinding interaction and preorganization of the trasition state with a reduction in the entropy of activation, in a manner analogous to enzyme catalysis. According to this geometric model, the enhancement in the 1–6 ring closure is dependent on the dimensional match between the zeolite cavity and the cyclic intermediate bringing the terminal carbons of *n*-hexane in close contact for C–C bond formation. In zeolites with different cavity geometries than LTL, adsorption of *n*-hexane results in a conformation less favorable for benzene formation.

Previously, it was shown that the ring closure ratio for conversion of *n*-hexane to benzene with Ir/K–LTL catalysts was similar to those reported here for Pt/K–LTL, despite the very much higher hydrogenolysis selectivity of Ir compared to Pt (33–35). Thus, the ring closure ratio appears to be independent of the properties of the metal and more a property of the zeolite type and pore geometry. In this study, Pt/K–LTL and Pt/K–MAZ displays ring closure ratios which are significantly higher than the other catalysts. It is noteworthy that MAZ is structurally similar to LTL in a number of details. Both zeolites have channels perpendicular to the [001] plane made up of cavities arranged linearly and connected through 7 Å windows. MAZ, however, has a smaller cavity diameter than LTL (9 Å in MAZ vs 11 Å in LTL). This structural similarity between LTL and MAZ is consistent with the proposal that the ring closure ratio is determined by the geometry of the zeolite support. This geometric contribution to the performance of the Pt/K–LTL catalyst by enhancement of 1–6 ring closure selectivity is consistent with the proposal that non-binding interactions between the *n*-paraffin adsorbate ad the pore walls leads to cyclic adsorption which resembles the transition state for formation of benzene.

Factors Contributing to Improved Dehydrocyclization Catalysts

For all catalysts, the ultimate benzene selectivity increases as the C_1–C_5 hydrogenolysis selectivity decreases, or the benezene selectivity increases. While there are many potential metal and support compositions for nonacidic dehydrocyclization catalysts, several factors including metal–support interaction, particle size and zeolite micropore geometry contribute to the high benzene yield of Pt/K–LTL. First, and most important, is the inherent, low C_1–C_5 hydrogenolysis selectivity of Pt compared to other metals. If the C_1–C_5 hydrogenolysis selectivity is high, as for example with Ir, none of the catalyst modifications can significantly improve the performance (33–35). For Pt, however, optimization of the metal–support interaction and the metal particle size lead to an additional small decrease in the C_1–C_5 hydrogenolysis selectivity. Changing the cation type of the zeolite or addition of a small excess of alkali over the ion exchange capacity leads to an increase in the platinum electron density resulting in a slightly lower C_1–C_5 hydrogenolysis selecivity. Furthermore, minimization of the Pt particle size may further lower the hydrogenolysis selectivity.

While electronic and particle size effects contribute to improved performance, an increase in the ring closure ratio also contributes to an increase in the aromatic selectivity. Of the known zeolite structures, the LTL geometry appears to have the highest 1–6 to 1–5 ring closure ratio. While the ring closure ratio is primarily determined by the support geometry, the ring closure ratio can also be increased slightly by addition of a small excess alkali to the support, i.e., an electronic effect. The direct effect of a high ring closure ratio is to increase the benzene yield. For the catalysts tested here, Pt/K–LTL produced 2–2.5 times more benzene at the same *n*-hexane conversion compared to catalysts with lower ring closure ratios. In addition to higher benzene selectivities, a high ring closure ratio also results in lower concentrations of 2-methylpentane and 3-methylpentane, i.e., the 1–5 ring closure products. These are also subject to hydrogenolysis, but without formation of benzene. Because of lower concentrations of these iso-hexanes, at high conversion of all hexanes a high ring closure ratio also leads to a reduction in the C_1–C_5 hydrogenolysis rate. In addition to increasing the aromatic selectivity, an increase in the ring closure ratio also increases the catalyst's apparent activity. As discussed, the rate of benzene formation from 2-methylpentane and 3-methylpentane is much slower than from *n*-hexane. Therefore, an increase in the ring closure ratio leads to lower concentrations of 2-methylpentane and 3-methylpentane, and thus requires less catalyst for high conversion of all hexanes.

Even for Pt catalysts on nonacidic supports, each of the catalyst modifications (electronic, particle size and geometric) are necessary for maximizing the benzene yield, and no one property is sufficient to ensure optimum performance. Failure to optimize any one property leads to a much less effective catalyst. For example, Pt/K–LTL (1.00) has small Pt particles on a nonacidic LTL support. Despite the high ring closure ratio and small Pt particles, the ultimate benzene selectivity is 0.77. By increasing the alkali level on the LTL zeolite, i.e., modification of the platinum electronic properties

through a metal–support interaction, the ultimate benzene selectivity increases to 0.93 due to a decrease in the C_1–C_5 hydrogenolysis selectivity and an increase in the ring closure ratio. Similarly, small Pt particles on FAU (1.11) have an ultimate benzene selectivity of 0.79. For this catalyst, the electronic properties of the support and the Pt particle size have been optimized, but the pore geometry has not. The low ring closure ratio of Pt/FAU leads to lower aromatic selectivity as demonstrated in the simulation. In summary, this study demonstrates that in addition to a metal with low C_1–C_5 hydrogenolysis selectivity and a non-acidic support, the most effective catalysts will have small metal particles and the support modified with alkali to optimize its electronic properties of the metal. Furthermore, the optimum catalyst will incorporate a support geometry which maximizes the ring closure ratio. The support which has the highest ring closure ratio is the LTL zeolite.

CONCLUSION

This study presents experimental results for several nonacidic supported platinum catalysts for the conversion of *n*-hexane to benzene and demonstrates the importance of the support geometry in controlling 1–6 to 1–5 ring closure selectivity. For most catalysts, including zeolite an amorphous supports, the ratio of 1–6 to 1–5 ring closure is similar at about 0.5. However, P/K–LTL catalysts exhibit a ring closure ratio greater than 1.0. P/K–MAZ, which has a pore geometry similar to that of LTL, was not quite as selective as Pt/K–LTL for 1–6 to 1–5 ring closure (0.89) but exhibited a higher ring closure ratio than the other catalysts. Addition of alkali above the ion-exchange capacity of the zeolite was also shown to result in a small increase in the ring closure selectivity and to be important in reduction of the C_1–C_5 hydrogenolysis selectivity.

These results were considered in light of many explanations that have been proposed to account for the high benzene yields of Pt/K–LTL catalysts. Proposals on the influence of support basicity, increased metal electron density, coke-free and small platinum particles, steric effects leading to reactant collimation (terminal adsorption) and preorganization of the transition state by cyclic adsorption on the zeolite were considered. While small metal particles and metal–support interactions leading to electron rich platinum particles are important for optimum performance, these explanations were insufficient to explain the high ring closure ratio of Pt/K–LTL. The experimental results also indicate that neither enhanced terminal adsorption, nor inhibition of coke by the zeolite pores correlates directly with a high 1–6 to 1–5 ring closure ratio. The experimental results are most consistent with the preorganization model, in which the reactant molecule is adsorbed in the zeolite channel in a cyclic conformation similar to the transition state, thereby reducing the entropy of activation leading to a preference for 1–6 ring closure. The zeolite geometry of LTL is best suited for this adsorption. MAZ, which is structurally similar to LTL, also shows an enhanced 1–6 ring closure supporting this explanation. The optimum catalyst is one with small platinum particles supported on the K–LTL zeolite that has been modified with a small excess of alkali.

The importance of the 1–6 to 1–5 ring closure ratio was demonstrated via computer simulations of the reaction pathway of *n*-hexane to benzene. The simulations demonstrate that at high conversion a high 1–6 to 1–5 ring closure ratio leads to a higher apparent activity. In addition, the ultimate benzene selectivity is substantially higher at high conversion leading to almost double the benzene yield at constant C_1–C_5 yield. These differences play a major role in the selection of a catalyst for commercial application and make the Pt/K–LTL catalyst the clear choice.

REFERENCES

1. Bernard, J. R., and Nury, J., U.S. Patent 4,104,320 to Elf France, 1978.
2. Bernard, J. R., *in* "Proc. 5th Int. Zeolite Conf." (L. V. C. Rees, Ed.), p. 686. Heyden, London, 1980.
3. Hughes, T. R., Buss, W. C., Tamm, P. W., and Jacobson, R. L., *in* "Studies in Surface Science and Catalysis," Vol. 28, New Developments in Zeolite Science and Technology, (Y. Murakami, A. Iijima, and J. Ward, Eds.), p. 725. Elsevier, Amsterdam, 1986.
4. Tamm, P. W., Mohr, D. H., and Wilson, C. R., *in* "Studies in Surface Science and Catalysis," Vol 38, Catalysis 1987 (J. W. Ward, Ed.), p. 335. Elsevier, Amsterdam, 1988.
5. *Oil Gas J.* **29** (Jan. 20, 1992).
6. Rotman, D., *Chemicalweek* **8** (Feb. 26, 1992).
7. Lane, G. S., Modica, F. S., and Miller, J. T., *J. Catal.* **129**, 145 (1991).
8. Mielczarski, E., Hong, S. B., Davis, R. J., and Davis, M. E., *J. Catal.* **134**, 359 (1992).
9. Larsen, G., and Haller, G. L., *Catal. Lett.* **3**, 103 (1989).
10. Sharma, S. B., Miller, J. T., and Dumesic, J. A., *J. Catal.* **148**, 198 (1994).
11. Besoukhanova, C., Guidot, J., Barthomeuf, D., Breysse, M., and Bernard, J. R., *J. Chem. Soc. Faraday Trans.* **77**, 1595 (1981).
12. de Mallmann, A., and Barthomeuf, D., *J. Chim. Phys.* **87**, 535 (1990).
13. Han, W.-H., Kooh, A. B., and Hicks, R. F., *Catal. Lett.* **18**, 193 (1993).
14. Han, W.-H., Kooh, A. B., and Hicks, R. F., *Catal. Lett.* **18**, 219 (1993).
15. Miller, J. T., Modica, F. S., Meyers, B. L., and Koningsberger, D. C., *Prep. Div. Pet. Chem. ACS* **38**, 825 (1993).
16. Mojet, B. L., Kappers, M. J., Muijsers, J. C., Niemantsverdriet, J. W., Miller, J. T., Modica, F. S., and Koningsberger, D. C., *in* "Studies in Surface Science and Catalysis," Vol. 84B, Zeolites and Related Microporous Materials: State of the Art 1994, (J. Weitkamp, H. G. Karge, H. Pfeifer, and W. Hölderich, Eds.), p. 909. Elsevier, Amsterdam, 1994.
17. Tauster, S. J., and Steger, J. J., *J. Catal.* **125**, 387 (1990).
18. Alvarez, W. E., and Resasco, D. E., *Catal. Lett.* **8**, 53 (1991).
19. Derouane, E. G., and Vanderveken, D. J., *Appl. Catal.* **45**, L15 (1988).
20. Davis, R. J., and Derouane, E. G., *Nature* **349**, 313 (1991).
21. Davis, R. J., and Derouane, E. G., *J. Catal.* **132**, 269 (1991).
22. Derouane, E. G., Julien-Lardoi, V., Davis, R. J., Blom, N., and Houjlund-Nielsen, P. E., *in* "Studies in Surface Science and Catalysis,"

Vol. 75B, New Frontiers in Catalysis (L. Guczi, F. Solymosi, and P. Tetenyi, Eds.), p. 1031. Elsevier, Amsterdam, 1993.
23. Iglesia, E., and Baumgartner, J. E., *in* "Studies in Surface Science and Catalysis," Vol. 75B, New Frontiers in Catalysis (L. Guczi, F. Solymosi, and P. Tetenyi, Eds.), p. 993. Elsevier, Amsterdam, 1993.
24. Jacobs, P. A., and Martens, J. A., *in* "Studies in Surface Science and Catalysis," Vol. 33, Synthesis of High-Silica Aluminosilicate Zeolites, p. 10. Elsevier, Amsterdam, 1987.
25. Argauer, R. J., and Landolt, G. R., (Mobil), U.S. Patent 3,702,886, 1972.
26. Jacobs, P. A., and Martens, J. A., *in* "Studies in Surface Science and Catalysis," Vol. 33, Synthesis of High-Silica Aluminosilicate Zeolites, p. 13. Elsevier, Amsterdam, 1987.
27. Perrotta, A. J., Kirby, C., Mitchell, B. R., and Tucci, E. R., *J. Catal.* **55**, 240 (1978).
28. Wadlinger, R. L., Kerr, G. T., and Rosinki, E. T., (Mobil), U.S. Patent 3,308,069, 1967.
29. Schaper, H., Berg-Slot, J. J., and Stork, W. H. J., *Appl. Catal.* **54**, 79 (1989).
30. Miller, J. T., Sajkowski, D. J., Modica, F. S., Lane, G. S., Gates, B. C., Vaarkamp, M., Grondelle, J. V., and Koningsberger, D. C., *Catal. Lett.* **6**, 369 (1990).
31. Karpinski, Z., Gandhi, S. N., and Sachtler, W. H. M., *J. Catal.* **141**, 337 (1993).
32. Mojet, B. L., Kappers, M. J., Miller, J. T., and Koningsberger, D. C., *in* "Studies in Surface Science and Catalysis," Vol. 101B, Proc. of the 11th ICC (J. W. Hightower, W. N. Delgass, E. Iglesia, and A. T. Bell, Eds.), p. 1165. Elsevier, Amsterdam, 1996.
33. Triantafillou, N. D., Miller, J. T., and Gates, B. C., *Prep. Div. Pet. Chem. ACS* **38**(4), 812 (1993).
34. Trinatiafillou, N. D., Miller, J. T., and Gates, B. C., *J. Catal.* **155**, 131 (1995).
35. Triantiafillou, N. D., Deutsch, S. E., Alexeev, O., Miller, J. T., and Gates, B. C., *J. Catal.* **159**, 14 (1996).